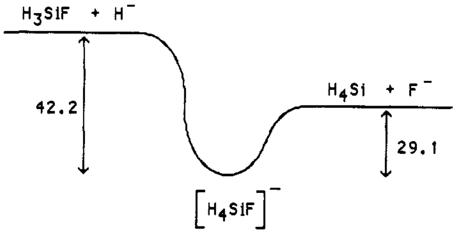

Figure 4. Ab initio energetics (kcal/mol) for formation of $[H_4SiF]^-$.

demonstrate that the computations presented in Table I can be used to predict the outcome of more complex reactions.

There are certain MNDO computations that do not fit our experimental results. One example is that of $[H_4SiF]^-$. Figure 3 depicts the energetics of $[H_4SiF]^-$ formation with the MNDO values. It indicates that reaction of H_3SiF and H^- should give this siliconate by analogy with our other successful direct siliconate syntheses from the endothermic side. Our experimental result is that the analogous methyl-substituted siliconate is made from $(CH_3)_3SiH$ and F^- (eq 8). Although MNDO gives a result irreconcilable with experiment, ab initio computations give a much more credible result (Figure 4). We see that reactions between H_4Si and F^- gives the siliconate, $[H_4SiF]^-$, which cannot escape through the substitution channel. Here is another example of MNDO calculations seriously underestimating the stability of the siliconate formed from a fluorosilane.

(8)

Other transfer reactions allow us to further probe the territory between computation and experiment. Transfer of F^- in reaction between $[H_3Si(CH_3)F]^-$ and H_3SiCl is predicted to be exothermic by 43 kcal/mol (29 kcal/mol by ab initio) (eq 9). The methyl-substituted reaction between $[(CH_3)_3Si(CH_3)F]^-$ and $(CH_3)_3SiCl$, however, gives no discernible $[(CH_3)_3SiFCl]^-$ even though $[(CH_3)_4SiF]^-$ rapidly reacts. On the other hand, reaction between $[H_3Si(CH_3)F]^-$ and H_4Si is exothermic by only 8 kcal/mol with MNDO (0.1 kcal/mol by ab initio). Experimentally, transfer between $[(CH_3)_3Si(CH_3)F]^-$ and $(CH_3)_3SiH$ gives a large signal for $[(CH_3)_3SiFH]^-$ (eq 10). Presumably, the first transfer is so exothermic that the siliconate product cannot be stabilized in the FA. When, as in the second case (eq 10), the transfer is less exothermic (a softer transfer), the product siliconate having a lower energy content can be stabilized and detected in the FA.

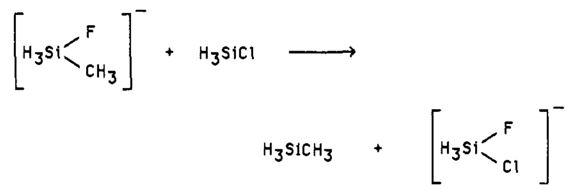

(9)

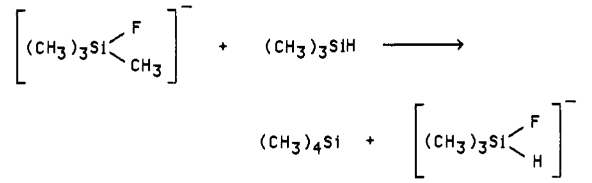

(10)

Acknowledgment. R.D. thanks the National Science Foundation (CHE-8519503 and CHE-8615808) for support of this work. Computer time used for the project was provided by the North Dakota State University Computer Center and by the San Diego Super Computer Center (through a grant from the National Science Foundation). M.S.G. was supported by the National Science Foundation (CHE-864077) and the Air Force Office of Scientific Research (AFOSR-870049).

Gas-Phase Chemistry of Transition Metal-Imido and -Nitrene Ion Complexes. Oxidative Addition of N-H Bonds in NH_3 and Transfer of NH from a Metal Center to an Alkene

Steven W. Buckner,[†] **James R. Gord,**[‡] **and Ben S. Freiser***

Contribution from the Herbert C. Brown Laboratory of Chemistry, Department of Chemistry, Purdue University, West Lafayette, Indiana 47907. *Received February 1, 1988*

Abstract: We report here on the gas-phase chemistry of a number of bare transition metal-nitrene and -imido ion complexes, MNH^+. Group 3, 4, and 5 atomic metal ions react with NH_3 at thermal energies to generate MNH^+ via dehydrogenation. A reaction mechanism is proposed involving initial oxidative addition to an N-H bond, in analogy to mechanisms proposed for reactions of gaseous atomic metal ions with hydrocarbons. Cr^+ reacts with NH_3 via slow condensation to form $CrNH_3^+$, as do all group 6-11 atomic metal ions investigated. However, excited-state Cr^+ reacts with NH_3 via bond-insertion reactions to form $CrNH_2^+$ and $CrNH^+$. An unidentified metastable electronic state of Cr^+, produced by direct laser desorption of chromium foil, reacts with much higher efficiency than does kinetically excited Cr^+. FeO^+ reacts with NH_3 to generate $FeNH^+$ with loss of H_2O. Thermochemical studies of VNH^+ and $FeNH^+$ involving ion-molecule reactions indicate values of $D°(V^+-NH) = 101 \pm 7$ kcal/mol and $D°(Fe^+-NH) = 54 \pm 14$ kcal/mol, the latter value in accord with $D°(Fe^+-NH) = 61 \pm 5$ kcal/mol obtained from photodissociation. The high bond strength for VNH^+ indicates multiple bonding, analogous to that in the isoelectronic VO^+, while the weaker bond strength for $FeNH^+$ indicates a single bond, analogous to that in the isoelectronic FeO^+. Proton-transfer experiments indicate $PA(VN) = 220 \pm 4$ kcal/mol from which $\Delta H_f(VN) = 111 \pm 9$ kcal/mol and $D°(V-N) = 125 \pm 9$ kcal/mol are obtained. VNH^+ is unreactive with ethene and benzene, but $FeNH^+$ transfers NH to ethene and benzene through metathesis and homologation reactions. A cyclic metalloaminobutane intermediate is consistent with the products of the $FeNH^+$/ethene reaction.

Studies have shown gas-phase atomic transition metal ions to be highly reactive species which exhibit many novel reaction pathways.[1] In particular, gas-phase atomic metal ions and highly unsaturated organometallic ions have been observed to activate

---

[†] Present address: Department of Chemistry, University of Arizona, Tucson, AZ 85721.

[‡] NSF predoctoral fellow.

(1) For a recent review of gas-phase metal-ion chemistry, see: Allison, J. In *Progress in Inorganic Chemistry*; Lippard, S. J., Ed.; Wiley-Interscience: New York, 1986; Vol. 34, p 628.

0002-7863/88/1510-6606$01.50/0

both C–H and C–C bonds in hydrocarbons, whereas metal complexes in solution activate C–H bonds exclusively. Activation of N–H bonds has been a topic of recent interest which prompted us to investigate the behavior of bare atomic metal ions with NH_3.

Activation of N–H bonds may be useful for catalytic functionalization of ammonia and amines.[2] However, only trinuclear osmium clusters and, recently, an Ir(I) complex have been observed to oxidatively add to N–H bonds of NH_3 in solution.[3,4] $CpTiC_5H_4TiCp_2$ and Cp_2MH_2 (M = Zr, Hf) have also been observed to react with NH_3 via a mechanism which may involve oxidative addition.[5] Allison and Radecki recently reported on the reactions of Co^+ with small amines in the gas phase where they provided evidence suggesting that Co^+ can insert into N–H bonds.[6] Here we report that early transition metal ions (groups 3–5) dehydrogenate NH_3 to form MNH^+. A mechanism is proposed for this reaction which involves initial oxidative addition of an N–H bond. The chemistry and thermochemistry of MNH^+ (M = V, Fe) is described in detail.

The chemistry of NR groups bound to transition metals has grown rapidly in recent years.[7] Complexes containing an MNR moiety are termed transition metal–imido or –nitrene, depending on whether the nitrogen is electron rich or electron deficient, respectively.[8,9] First-row transition metal–imido complexes for electron-rich metals are relatively rare in solution, and their chemistry has not been investigated in detail. The interest in the NH group is due to its role in homogeneous and heterogeneous catalysis. The NH group is most often multiply bonded to the metal center, making transfer from the metal center to another molecule difficult. Recent results on a ruthenium trinuclear center having a bridging NPh group, however, indicate coupling of CO and alkynes to the NPh, reaction 1.[10]

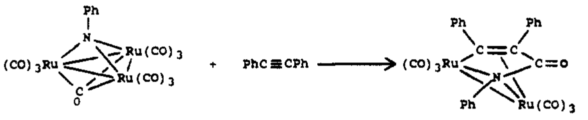

+ other products (1)

In this study, $FeNH^+$ was observed to react with olefins in the gas phase by transfer of NH to the olefin. This reaction is proposed to proceed through a four-centered intermediate.

Experimental Section

All experiments were performed on a prototype Nicolet FTMS-1000 Fourier transform mass spectrometer[11] equipped with a 5.2-cm cubic trapping cell situated between the poles of a Varian 15-in. electromagnet maintained at 0.9 T. The transmitter plates on the cell have been replaced by 80% transmittance screens to allow irradiation of the ions with an arc lamp. The screens only decrease the detected ion current by a small amount. Typical operating parameters were as follows: trapping voltages, 2.5 V; number of data points, 16K; mass range, 20 → 1K amu. Product ion distributions reported are reproducible to within ±10% absolute.

Metal ions were produced by pulsed laser desorption/ionization using the fundamental output (1064 nm) of a pulsed Quanta Ray Nd:YAG laser focussed onto a pure metal foil. Laser desorption for production of atomic metal ions has previously been discussed in detail.[12]

Table I. New Thermochemical Values (See Text)

$D°(M^+–NH) > 93$ kcal/mol	(M = Sc, Ti, Y, Zr, Nb, La, Ta)
$D°(V^+–NH) = 101 \pm 7$ kcal/mol	
$D°(V–N) = 125 \pm 10$ kcal/mol	
$D°(Fe^+–NH) = 54 \pm 14$ kcal/mol	
$D°(V^+–C_3H_5) = 102 \pm 16$ kcal/mol	

Chemicals were obtained commercially in high purity and used as supplied except for multiple freeze–pump–thaw cycles to remove noncondensable gases. Reagents for synthesis of MNH^+ (NH_3 and N_2O) were introduced into the vacuum system through a General Valve Corp. series 9 pulsed solenoid valve.[13] The pressure in the cell after firing the pulsed valve was on the order of 10^{-4} torr. The reagent was pumped away (after ~400 ms) prior to isolation of the product ions by swept double resonance ejection pulses. For synthesis of $FeNH^+$, a second pulsed valve recently installed on our instrument was used. Swept double resonance ejection pulses were used to isolate $FeNH^+$ prior to reaction.[14] Other reagent gases (ethylene, bases) were admitted into the cell at a static background pressure of $\sim 6 \times 10^{-7}$ torr. Argon was maintained at a static background pressure of $\sim 2 \times 10^{-5}$ torr to help thermalize any kinetically excited ions and to act as a collision gas for collision-induced dissociation (CID).[15] Pressures were measured using an uncalibrated Bayard-Alpert ionization gauge. The FTMS–CID experiment is a multicollision experiment which allows rearrangements to occur prior to detection.[16] Thus, while CID has been demonstrated to be an excellent structural tool for some small metal–ligand ions, CID results are not conclusive in and of themselves and additional techniques are required for absolute structural identification.

Discussion

Formation and Bonding in MNH^+. Bare atomic transition metal ions (groups 3–5) react with NH_3 by dehydrogenation, reaction 2. Observation of exothermic dehydrogenation of NH_3 indicates

$$M^+ + NH_3 \rightarrow MNH^+ + H_2 \qquad (2)$$

$$M = \text{Sc, Ti, V, Y, Zr, Nb, La, Ta}$$

$D°(M^+–NH) > 93$ kcal/mol.[17] Table I lists new thermochemical data obtained in this study.

V^+ also forms a small amount of the direct attachment product, VNH_3^+, the ratio of VNH^+/VNH_3^+ formation being dependent on the pressure in the cell. Using the highest pressures in our instrument during pulsed valve addition of reagent, $\sim 1 \times 10^{-4}$ torr, VNH_3^+ is ~10% as intense as VNH^+. Preliminary results from Squires and co-workers indicate V^+ forms only the attachment product in reaction with NH_3 at 0.75 torr of He in a flowing afterglow.[18]

VNH_3^+ was prepared in high yield in our instrument by displacing isobutene from $VC_4H_8^+$, reactions 3 and 4. The VNH_3^+

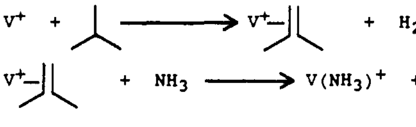

(3)

(4)

prepared by reaction 4 should be relatively cool. CID of VNH_3^+ yields only loss of NH_3, reaction 5. This is in contrast to the

$$V(NH_3)^+ \xrightarrow{Ar} V^+ + NH_3 \qquad (5)$$

---

[2] (a) Yamamoto, Y.; Yatagai, H.; Murayami, K. *J. Chem. Soc., Chem. Commun.* **1980**, 835. (b) Hedden, D.; Roundhill, D. M.; Fultz, W. C.; Rheingold, A. L. *J. Am. Chem. Soc.* **1984**, *106*, 5014.

[3] (a) Johnson, B. F. G.; Lewis, J.; Odiaka, T. I.; Raithby, P. R. *J. Organomet. Chem.* **1981**, *216*, c56. (b) Bryan, E. G.; Johnson, B. F. G.; Lewis, J. *J. Chem. Soc. Dalton* **1977**, 1328.

[4] Casalnuovo, A. L.; Calabrese, J. C.; Milstein, D. *Inorg. Chem.* **1987**, *26*, 973.

[5] (a) Armor, J. N. *Inorg. Chem.* **1978**, *17*, 203. (b) Hillhouse, G. L.; Bercaw, J. E. *J. Am. Chem. Soc.* **1984**, *106*, 5472.

[6] Allison, J.; Radecki, B. D. *J. Am. Chem. Soc.* **1984**, *106*, 946.

[7] (a) Sharp, P. R.; Ge, Y. W. *J. Am. Chem. Soc.* **1987**, *109*, 3796. (b) Lahiri, G. K.; Goswami, S.; Falvello, L. R.; Chakravorty, A. *Inorg. Chem.* **1987**, *26*, 3365. (c) Curtis, M. D.; D'Errico, J. J.; Butler, W. M. *Organometallics* **1987**, *6*, 2151.

[8] Basolo, F. *J. Indian Chem. Soc.* **1977**, *54*, 7.

[9] Nugent, W. A.; Haymore, B. L. *Coord. Chem. Rev.* **1980**, *31*, 123.

[10] (a) Han, S.; Geoffroy, G. L.; Rheingold, A. L. *Organometallics* **1987**, *6*, 2380. (b) Han, S.; Geoffroy, G. L.; Rheingold, A. L. *Inorg. Chem.* **1987**, *26*, 3426.

[11] Comisarow, M. B.; Marshall, A. G. *Chem. Phys. Lett.* **1974**, *26*, 489. (b) Freiser, B. S. *Talanta* **1985**, *32*, 697.

[12] Cody, R. B.; Burnier, R. C.; Reents, W. D., Jr.; Carlin, T. J.; McCrery, D. A.; Lengel, R. K.; Freiser, B. S. *Int. J. Mass Spectrom. Ion Phys.* **1980**, *33*, 37.

[13] Carlin, T. J.; Freiser, B. S. *Anal. Chem.* **1983**, *55*, 571.

[14] Comisarow, M. B.; Parisod, G.; Grassi, V. *Chem. Phys. Lett.* **1978**, *57*, 413.

[15] Cody, R. B.; Freiser, B. S. *Int. J. Mass Spectrom. Ion Phys.* **1982**, *41*, 199.

[16] Jacobson, D. B.; Freiser, B. S. *J. Am. Chem. Soc.* **1983**, *105*, 7484.

[17] Supplementary thermochemical information taken from: Rosenstock, H. M.; Draxl, D.; Steiner, B. W.; Herron, J. T. *J. Phys. Chem. Ref. Data, Suppl. 1* **1977**, *6*.

[18] Marinelli, P.; Squires, R. R., in preparation.

Scheme I

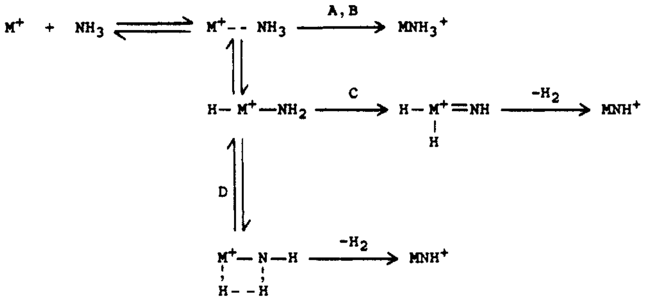

A - STABILIZING 3rd BODY COLLISION
B - IR RADIATIVE RELAXATION
C - α-H MIGRATION (ROUTE 1)
D - ROUTE 2

results of reaction 2; however, differences in products observed from collisional activation of metal–ligand ions and those observed for ion–molecule reactions of the metal ion with the corresponding neutral ligand have previously been observed.[16]

In our instrument, reactions 6 and 7 are slow (on the order of 5% of the collision frequency), which could indicate reaction 6 is thermoneutral or slightly endothermic. To test this, VNH$^+$

$$V^+ + NH_3 \rightarrow VNH^+ + H_2\ (99\%) \quad (6)$$
$$ \rightarrow VNH_3^+\ (1\%) \quad (7)$$

was isolated and trapped in 8 × 10^{-7} torr of H_2 for 1 s. V$^+$ was not regenerated, reaction 8, indicating that $D°(V^+–NH) > 93$ kcal/mol is a good lower limit.

$$VNH^+ + H_2 \not\rightarrow V^+ + NH_3 \quad (8)$$

VNH$^+$ undergoes CID via loss of H$^•$ and NH, reactions 9 and 10. These results indicate α-hydrogen migration is facile for V$^+$. A mechanism for reaction 2 is shown in Scheme I, which involves

$$VNH^+ \xrightarrow{Ar} VN^+ + H^• \quad (9)$$
$$\phantom{VNH^+ \xrightarrow{Ar}} \rightarrow V^+ + NH \quad (10)$$

initial coordination of NH_3 to the metal center followed by oxidative addition to an N–H bond. The intermediate hydrido–amido–metal ion complex can undergo α-hydrogen migration onto the metal center followed by reductive elimination of H_2 (route 1). Alternatively, the hydrido–amido–metal ion complex can eliminate H_2 via a four-centered intermediate (route 2). Oxidative addition to N–H bonds is rare for transition metal complexes in solution.[2] Os_3 clusters have been observed to oxidatively add to N–H bonds in primary amines, reaction 11;[3] a mechanism has

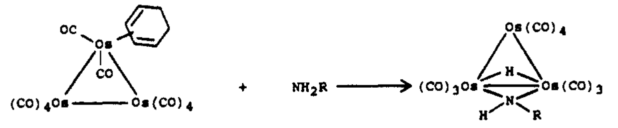

+ other products (11)

been proposed in which Rh(I) oxidatively adds to an N–H bond in *n*-butylamine,[2a] and recently an Ir(I) complex has been observed to undergo oxidative addition to an N–H bond.[2b] Recently, Casalnuovo, Calabrese, and Milstein have observed oxidative addition of N–H bonds in NH_3 and aniline to $Ir(PEt_3)_2(C_2H_4)_2Cl$.[4,19] Allison and Radecki have presented evidence which strongly suggests that gas-phase Co$^+$ inserts into N–H bonds in amines.[6] The present results indicate that oxidative addition of an N–H bond to a bare metal center in the gas phase is quite facile, in contrast to the behavior of complexes in solution. These results support the earlier findings of Radecki and Allison.

VNH$^+$ is extremely reactive with oxygen-containing compounds. All mass spectra for formation or subsequent reaction of VNH$^+$ contain a VO$^+$ peak due to reaction of VNH$^+$ with background H_2O and O_2, reactions 12 and 13. VO$^+$ and VNH$_2^+$ have the

$$VNH^+ + H_2O \rightarrow VO^+ + NH_3 \quad (12)$$

$$VNH^+ + O_2 \rightarrow VO^+ + HNO \quad (13)$$

same nominal mass, *m/z* 67 amu. At a resolution of 2800, only a singlet was observed at the mass of VO$^+$. The VO$^+$ is also due to the reaction of V$^+$ with background O_2 and H_2O, which occurs at a rate near the Langevin frequency.[20] Observation of reaction 13 implies $D°(V^+–NH) < 127$ kcal/mol, while reaction 12 implies $D°(V^+–NH) < 100 \pm 6$ kcal/mol. The limit from reaction 12 combined with the limit from reactions 6 and 8 indicates $D°(V^+–NH) = 100 \pm 7$ kcal/mol. This high bond strength suggests multiple bonding in analogy to the isoelectronic VO$^+$, which also has a high bond strength, 131 ± 4 kcal/mol, and is proposed to have a triple bond.[21]

Table II. Proton-Transfer Reactions of VNH$^+$: $VNH^+ + B \rightarrow BH^+ + VN$

B	PA (kcal/mol)[a]	transfer obsd
ammonia	205	no
sec-butylamine	217	no
pyridine	218.1	no
n-propylamine	218.5	no
diethylamine	222.7	yes
triethylamine	231	yes

[a] Values obtained from ref 17.

Proton-transfer reactions were performed with VNH$^+$ and various bases.[22] The presence or absence of protonated base in reaction 14 was noted for determining the proton affinity of VN,

$$VNH^+ + B \rightarrow VN + BH^+ \quad (14)$$
$$B = \text{various bases}$$

(i.e., yes/no bracketing methods); see Table II. Complicating side reactions occurred for the bases used, but it is believed that the liberal error brackets, along with the variety of bases used, gives an accurate value. From PA(VN) = 220 ± 6 kcal/mol, a value of $\Delta H_f(VN) = 111 \pm 9$ kcal/mol is obtained which yields $D°(V–N) = 125 \pm 9$ kcal/mol.

Cr$^+$, like all other first-row group 6–11 transition metal ions, reacts at thermal energies only via formation of CrNH$_3^+$. However, directly after formation, laser desorbed Cr$^+$ reacts with NH_3 by reactions 15–17. Laser desorption of metal surfaces at

$$Cr^+ + NH_3 \rightarrow CrNH^+ + H_2 \quad (15)$$
$$ \rightarrow CrNH_2^+ + H^• \quad (16)$$
$$ \rightarrow CrNH_3^+ \quad (17)$$

the high powers (10^8 W/cm^2) used in the present experiments has been shown to produce electronically[23] and kinetically[24] excited metal ions. If the laser desorbed Cr$^+$ is trapped in a high pressure of argon (~2 × 10^{-5} torr) and reisolated after 1 s, only reaction 17 is observed. If the cooled Cr$^+$ is excited by an rf pulse at its cyclotron frequency, reactions 15 and 16 are again observed.[25] Directly laser desorbed Cr$^+$ produces ~0–4% of reactions 15 and 16 (owing to day-to-day fluctuations in laser power), whereas the kinetically excited Cr$^+$ forms <0.1% over the entire energy range studied (0–140 eV laboratory collision energy). The much higher efficiency toward bond insertion reactions for the laser desorbed Cr$^+$ indicates that an electronically excited state of Cr$^+$ is involved. The millisecond time scale between collisions in our experiment

---

(19) Casalnuovo, A. L.; Calabrese, J. C.; Milstein, D. *J. Am. Chem. Soc.*, submitted for publication.

(20) Su, T.; Bowers, M. T. In *Gas Phase Ion Chemistry*; Bowers, M. T., Ed.; Academic: New York, 1979; Vol. 1, pp 83–118.

(21) Aristov, N.; Armentrout, P. B. *J. Am. Chem. Soc.* **1984**, *106*, 4065.

(22) Proton affinity values taken from: Hartmann, K. N.; Lias, S.; Ausloos, P.; Rosenstock, H. M.; Schroyer, S. S.; Schmidt, C.; Martinson, D.; Milne, G. W. A. *A Compendium of Gas Phase Basicity and Proton Affinity Measurements*; National Bureau of Standards: Washington, D.C., 1977.

(23) Buckner, S. W.; Freiser, B. S. *J. Am. Chem. Soc.* **1987**, *109*, 1247.

(24) Kang, H.; Beauchamp, J. L. *J. Phys. Chem.* **1985**, *89*, 3364.

(25) Bensimon, M.; Houriet, R. *Int. J. Mass Spectrom. Ion Phys.* **1986**, *72*, 93. (b) Forbes, R. A.; Lech, L. M.; Freiser, B. S. *Int. J. Mass Spec. Ion Processes* **1987**, *77*, 107.

Scheme II

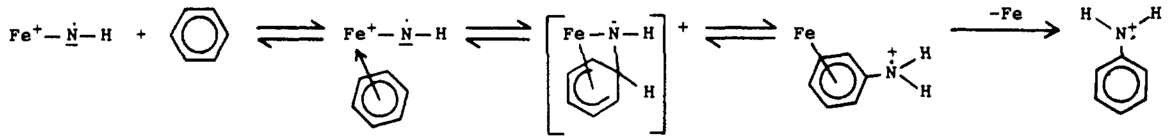

requires that the electronic state be metastable in order to live long enough to undergo a reactive collision. Previously, $(Cr^+)^*$ in an unidentified metastable state generated by electron impact on $Cr(CO)_6$ was observed to react with CH_4 to form $CrCH_2^+$.[26] The higher reaction efficiency of electronically excited metal ions relative to kinetically excited metal ions has recently been observed by Weisshaar and co-workers in the reaction of V^+ with C_2H_6, where the a^3F state reacts with >200 times the efficiency of kinetically excited V^+.[27] Similarly, Aristov and Armentrout have recently shown that electronic excitation of V^+ greatly enhances the reaction cross sections with methane.[28] If oxidative addition is occurring in the reaction of $(Cr^+)^*$ with NH_3, then the $3d^44s^1$ electronic configuration may be responsible for the bond insertion reactions.

The $CrNH_2^+$ produced in reaction 16 would have a primary amide structure, $Cr^+{-}NH_2$, if the reaction proceeds via oxidative addition. Primary amide complexes for electron-rich metals are extremely rare. This has previously been attributed to the unfavorable interaction of the lone pair on the nitrogen with the valence electrons on the metal center which would produce a weak $M{-}NH_2$ bond.[29] However, we have recently shown $Fe^+{-}NH_2$ and $Co^+{-}NH_2$ have relatively high bond strengths.[30]

Though thermal bare atomic metal ions of groups 6–11 react slowly with NH_3 to form only MNH_3^+, selected ligated metal ions in these groups react rapidly with NH_3 via bond-insertion processes. For example, $FeOH^+$ and $CoOH^+$ react with NH_3 as in reaction 18. In a similar reaction, FeO^+, produced in reaction

$$MOH^+ + NH_3 \rightarrow MNH_2^+ + H_2O \qquad (18)$$

19, reacts with NH_3 via reaction 20. Deprotonation of primary

$$Fe^+ + N_2O \rightarrow FeO^+ + N_2 \qquad (19)$$

$$FeO^+ + NH_3 \rightarrow FeNH^+ + H_2O \qquad (20)$$

amines is the most frequent method for synthesis of metal–imido complexes in solution, as exemplified by reaction 21. This method

$$ReOCl_3(PEt_2Ph)_2 + PhNH_2 \xrightarrow{\text{benzene}} Re(NPh)Cl_3(PEt_2Ph)_2 + H_2O \qquad (21)$$

is analogous to reaction 20.[9,31] Based on $D°(Fe^+{-}O) = 68 \pm 3$ kcal/mol reported previously,[32] reaction 20 implies $D°(Fe^+{-}NH) > 41$ kcal/mol. An attempt to displace NH from $FeNH^+$ with benzene was unsuccessful as only reaction 22 was observed. The

$$FeNH^+ + c\text{-}C_6H_6 \rightarrow [C_6H_5NH_2]^+ + Fe \qquad (22)$$

transfer of an NR group from a metal center to another molecule has been a difficult but important goal of transition metal imido chemistry. The high stability of the M–N bond in these complexes afforded by multiple bonding is responsible for the difficulty in transferring the NR group.[9] Thus, reaction 22 is an interesting example of NH transfer. A mechanism consistent with these results is shown in Scheme II.

Scheme III

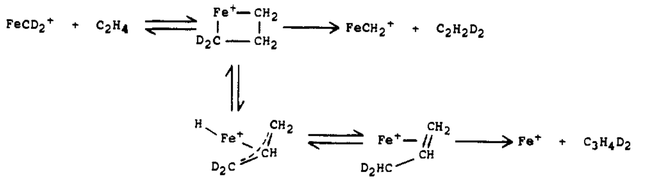

$FeNH^+$ reacts with O_2 to produce FeO^+, reaction 23, which indicates $D°(Fe^+{-}NH) < 65 \pm 3$ kcal/mol from $\Delta H_f(HNO) =$

$$FeNH^+ + O_2 \rightarrow FeO^+ + HNO \qquad (23)$$

24.6 kcal/mol reported previously.[33] The limits from reactions 20 and 23 yield 41 kcal/mol $< D°(Fe^+{-}NH) <$ 68 kcal/mol, in agreement with $D°(Fe^+{-}NH) = 61 \pm 5$ kcal/mol obtained from a photodissociation threshold measurement.[34] This relatively low bond strength indicates $Fe^+{-}NH$ may be singly bonded, in analogy to the bonding proposed for the isoelectronic $Fe^+{-}O$,[35a] which also has a relatively low bond strength, ~68 kcal/mol.

Recently, Armentrout and co-workers have found that by plotting the metal ion–ligand bond strength versus the bond strength of the corresponding carbon analogue, as in Figure 1, a linear relationship is observed with distinct regions observed on the line corresponding to single, double, and triple bonds.[21] Although these plots are highly speculative, and full theoretical calculations are necessary for a detailed understanding of the bonding in these systems, they provide a qualitative picture of the bonding in these very complicated transition metal systems. Figure 1a shows the correlation for $V^+{-}L$, with the majority of the points from work by Aristov and Armentrout. In this plot VNH^+ correlates with a double bond. Multiple bonding occurs for early transition metal oxides because the empty $d\pi$ orbitals on the metal can accept electron density from the oxygen.[35b] Similarly, early transition metal ions can accept back-donation from the $p\pi$ electrons on the nitrogen in the NH group. Figure 1b shows the correlation plot for $Fe^+{-}L$. In this case $FeNH^+$ lies in the single bond region, as does FeO^+. For Fe^+, Co^+, and Ni^+, single bonds are expected because of the filled orbitals on the metal center which cannot accept electron density from the $p\pi$ orbitals on the oxygen or on the NH group. Figure 1c demonstrates that the "Armentrout plot" can also be applied with success to study neutral metal atom–ligand bond strengths for vanadium. In this case it is impossible to define distinct bonding regions owing to the paucity of data points on the plot. However, it is clear that V–N falls into a multiple bonding region, somewhere between a double and a triple bond.

MNH species are called either imido complexes or nitrene complexes depending on whether the NH group is electron rich or deficient, respectively.[8,9] For nitrene complexes there is extensive multiple bonding due to donation from the nitrogen to the metal center. This is what appears to be occurring for the VNH^+ case, structure I. For imido complexes, the electron density is

$$\begin{array}{cc} V^+{=}\bar{N}{-}H & Fe^+{-}\bar{N}{-}H \\ \text{nitrene (N-electron deficient)} & \text{imido (N-electron rich)} \\ \text{I} & \text{II} \end{array}$$

localized more on the nitrogen, as in the $FeNH^+$ case, structure II. These structures are also consistent with the reactivity patterns for VNH^+ and $FeNH^+$ with alkenes as discussed below. However,

---

(26) (a) Freas, R. B.; Ridge, D. P. *J. Am. Chem. Soc.* **1980**, *102*, 7129. (b) Reents, W. D., Jr.; Strobel, F.; Freas, R. B.; Wronka, J.; Ridge, D. P. *J. Phys. Chem.* **1985**, *89*, 5666. (c) Schilling, J. B.; Beauchamp, J. L. *Organometallics* **1988**, *7*, 194.

(27) Sanders, L.; Hanton, S.; Weisshaar, J. C. *J. Phys. Chem.* **1987**, *91*, 5145.

(28) Aristov, N.; Armentrout, P. B. *J. Phys. Chem.* **1987**, *91*, 6178.

(29) Lappert, M. F.; Power, P. P.; Sanger, A. R.; Srivastava, R. C. *Metal and Metalloid Amides*; Ellis Horwood: West Sussex, England, 1980.

(30) Buckner, S. W.; Freiser, B. S. *J. Am. Chem. Soc.* **1987**, *109*, 4715.

(31) Chatt, J.; Rowe, G. A. *J. Chem. Soc. Dalton Trans.* **1959**, 705.

(32) Armentrout, P. B.; Halle, L. F.; Beauchamp, J. L. *J. Am. Chem. Soc.* **1981**, *103*, 6501.

(33) Karapet'Yants, M. K. *Thermodynamic Constants of Inorganic and Organic Compounds*; Ann Arbor Humphrey Science Publishers: Ann Arbor, MI, 1970.

(34) MacMahon, T. J.; Freiser, B. S., unpublished results.

(35) (a) Hettich, R. L. Ph.D. Thesis, Purdue University, 1986. (b) Hettich, R. L.; Freiser, B. S. *J. Am. Chem. Soc.* **1987**, *109*, 3543.

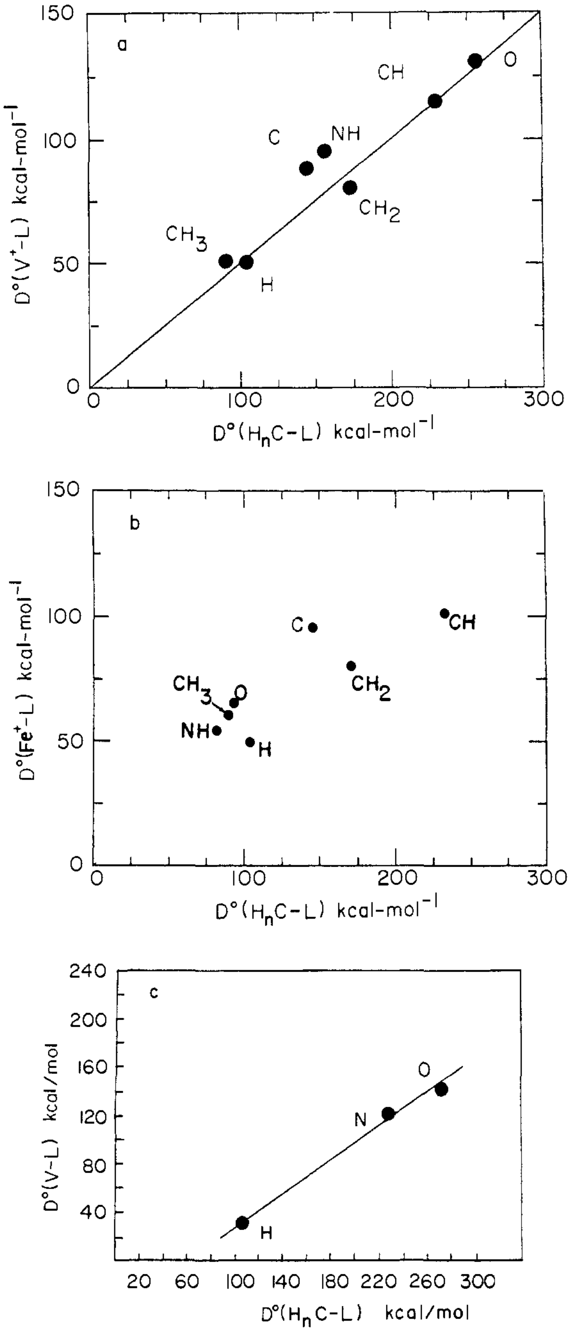

Figure 1. (a) Correlation of VL^+ bond dissociation energies with those for the corresponding carbon analogues (CH_n–L). (b) Correlation of FeL^+ bond dissociation energies with those for the corresponding carbon analogues. (c) Correlation of VL bond dissociation energies with those for the corresponding carbon analogues.

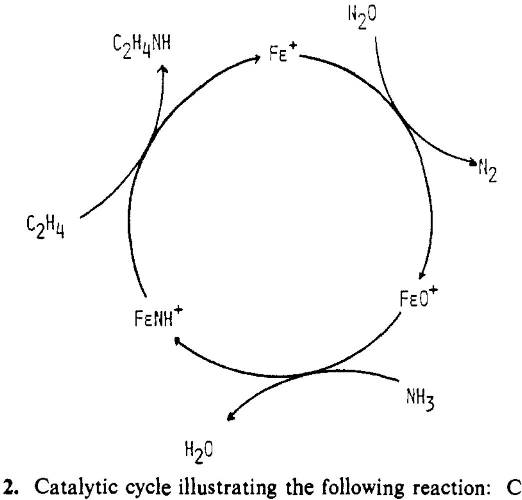

Figure 2. Catalytic cycle illustrating the following reaction: $C_2H_4 + NH_3 + N_2O\ (+Fe^+) \rightarrow C_2H_4NH + H_2O + N_2$.

Scheme IV

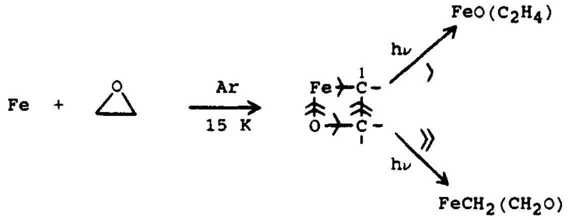

in the absence of spectroscopic information or high-level calculations, the bonding proposed is clearly speculative.

Reactions with Ethylene. VNH^+ is unreactive with ethylene (eq 24), but $FeNH^+$ reacts to produce a variety of products.

$$VNH^+ + C_2H_4 \rightarrow NR \qquad (24)$$

Reactions 25 and 26 provide additional examples of NH transfer,

$$FeNH^+ + C_2H_4 \rightarrow Fe^+ + C_2H_4NH \ (38\%) \qquad (25)$$
$$\rightarrow FeCH_2^+ + CH_2NH \ (19\%) \qquad (26)$$
$$\rightarrow Fe(NH_3)^+ + C_2H_2 \ (16\%) \qquad (27)$$
$$\rightarrow Fe(HCN)^+ + CH_4 \ (15\%) \qquad (28)$$
$$\rightarrow FeNH(C_2H_2)^+ + H_2 \ (12\%) \qquad (29)$$

similar to reaction 22 with benzene. In addition, reactions 25 and 26 are analogous to those observed in the reactions of $FeCH_2^+$ with ethylene, where a metathesis reaction was proposed to proceed through a four-centered metallocyclic intermediate, Scheme III.[36] Furthermore, a metallaoxetane of iron has recently been reported by Margrave and co-workers in a matrix reaction between the metal atoms and ethylene oxide.[37] The metallaoxetanes undergo photochemical decomposition as in Scheme IV. A similar intermediate is very likely for the present reactions. Scheme V shows initial coordination of ethylene to the metal center. After π-donation to the metal center, the ethylene becomes partially positive, activating it toward nucleophilic attack by the electron-rich nitrogen. Theoretical discussions by Eisenstein and Hoffmann have indicated η^2-coordinated olefins are actually deactivated toward nucleophilic attack, but slippage of the olefin to η^1-coordination activates the olefin toward nucleophilic attack.[38] The four-centered intermediate can regenerate $FeNH^+$ by loss of ethylene, or form the other metathesis products, $FeCH_2^+$ and CH_2NH. Alternatively, a β-hydrogen shift from the metallocycle, followed by a H• migration from the metal center to the terminal carbon and elimination of C_2H_4NH accounts for the homologation product. Formation of $Fe(HCN)^+$ requires insertion into a C–C bond with subsequent elimination of CH_4. Combining reactions 19, 20, and 25 completes an Fe^+ "catalyzed" cycle for generation of a C–N bond from NH_3 and ethylene, Figure 2. Side reactions in the $FeNH^+$/ethylene step interfere, but the cycle represents the main product.

FeO^+ reacts with ethylene as in reactions 30–33.[39] These reaction products are analogous to those observed for the $FeNH^+/C_2H_4$ reaction as well as the $FeCH_2^+/C_2H_4$ reaction.

$$FeO^+ + C_2H_4 \rightarrow Fe^+ + C_2H_4O \ (82\%) \qquad (30)$$
$$\rightarrow FeCH_2^+ + CH_2O \ (11\%) \qquad (31)$$
$$\rightarrow FeC_2H_2^+ + H_2O \ (4\%) \qquad (32)$$
$$\rightarrow FeCO^+ + CH_4 \ (3\%) \qquad (33)$$

Thus, the three isoelectronic species $FeCH_2^+$, FeO^+, and $FeNH^+$ all react with ethylene to generate similar products, suggesting the generalized mechanism shown in Scheme VI. Scheme VII shows an alternative route for the formation of $FeC_2H_2^+$.

---

(36) Jacobson, D. B.; Freiser, B. S. *J. Am. Chem. Soc.* **1985**, *107*, 2605.

(37) Kafafi, Z. H.; Hauge, R. H.; Billups, W. E.; Margrave, J. L. *J. Am. Chem. Soc.* **1987**, *109*, 4775.

(38) Eisenstein, O.; Hoffmann, R. *J. Am. Chem. Soc.* **1981**, *103*, 4308.

(39) Jackson, T. C. Ph.D. Thesis, Purdue University, 1985.

Scheme V

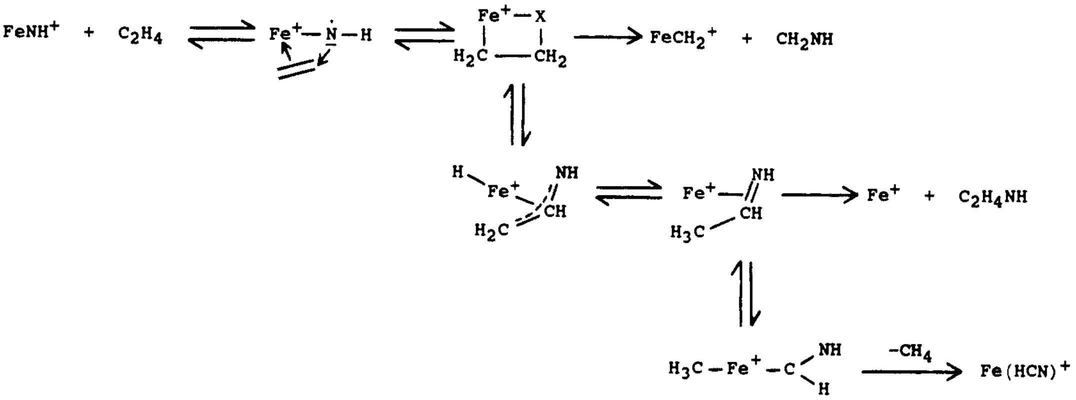

Scheme VI

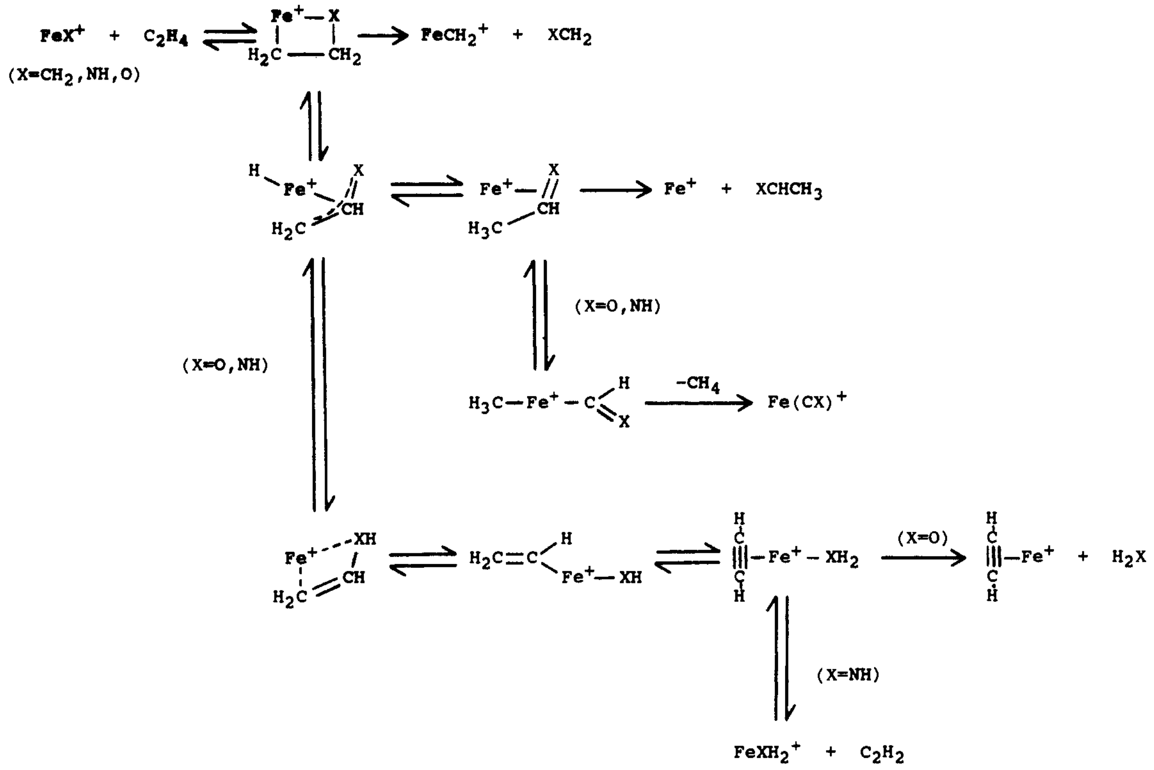

Scheme VII

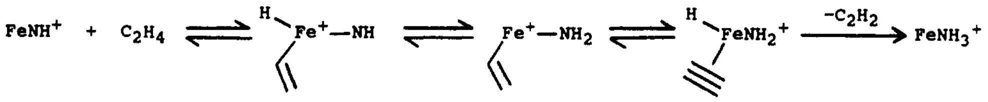

V^+ reacts with hydrocarbons predominantly by activating C–H bonds, eliminating H_2, and forming $V(alkene)^+$ complexes.[40] The reactivity of VO^+, however, is greatly reduced. This pattern is also observed for other early transition metal oxide ions with high bond strengths, including LaO^+, NbO^+, and TaO^+, and may be due to electronic saturation by these very tightly bound ligands.[41] In contrast, VNH^+ reacts with propene at twice the rate of V^+ (only relative rates were determined), reactions 34–39. Reaction 36 implies $D°(V^+–C_3H_5) > 87$ kcal/mol. From this and $D°(V^+–C_3H_5) < 118$ kcal/mol, obtained recently in a study of the reaction of V^+ with propane,[40] a value of 102 ± 16 kcal/mol is assigned.

$VO^+ + \text{propene} \rightarrow \text{NR}$ (34)

$V^+ + \text{propene} \rightarrow VC_3H_4^+ + H_2$ (86%) (35)

$\rightarrow VC_3H_5^+ + H^\bullet$ (14%) (36)

$VNH^+ + \text{propene} \rightarrow VNH(C_3H_4)^+ + H_2$ (62%) (37)

$\rightarrow VC_2NH_6^+ + CH$ (5%) (38)

$\rightarrow VCH_2NH^+ + C_2H_4$ (33%) (39)

Although $FeNH^+$ transfers an NH group to ethylene, VNH^+ is not observed to transfer NH in any of its reactions. This can be attributed to the significantly higher bond strength of V^+–NH which renders these pathways endothermic.

Acknowledgment is made to the Division of Chemical Sciences, Office of Basic Energy Sciences, U.S. Department of Energy (DE-FG02-87ER13766), for supporting the transition metal ion research and to the National Science Foundation (CHE-8612234) for the continued support of the Fourier transform mass spectrometry instrumentation. S.W.B. acknowledges the W. R. Grace foundation for fellowship support. J.R.G. acknowledges the National Science Foundation for providing predoctoral fellowship support. We also thank Professor R. R. Squires and Pete Marinelli for communicating their preliminary results.

---

(40) Jackson, T. C.; Freiser, B. S. *J. Am. Chem. Soc.* **1986**, *108*, 1102.

(41) Buckner, S. W.; Huang, Y.; Freiser, B. S., unpublished results.

Registry No. H$^+$, 12408-02-5; NH, 13774-92-0; N$^-$, 18851-77-9; Sc$^+$, 14336-93-7; Ti$^+$, 14067-04-0; Y$^+$, 14782-34-4; Zr$^+$, 14701-19-0; Nb$^+$, 18587-63-8; La$^+$, 14175-57-6; Ta$^+$, 20561-66-4; V$^+$, 14782-33-3; Fe$^+$, 14067-02-8; Sc$^+$-NH, 115858-87-2; Ti$^+$-NH, 115858-88-3; Y$^+$-NH, 115858-89-4; Zr$^+$-NH, 115858-90-7; Nb$^+$-NH, 115858-91-8; La$^+$-NH, 115858-92-9; Ta$^+$-NH, 115858-93-0; V$^+$-NH, 115858-94-1; Fe$^+$-NH, 115858-95-2; V$^+$-C_3H_5, 115858-96-3; V-N, 24646-85-3; Cr$^+$, 14067-03-9; c-C_6H_6, 71-43-2; O_2, 7782-44-7; C_2H_4, 74-85-1; propene, 115-07-1; ammonia, 7664-41-7; *sec*-butylamine, 13952-84-6; *n*-propylamine, 107-10-8; pyridine, 110-86-1; diethylamine, 109-89-7; triethylamine, 121-44-8.

Surface-Enhanced Raman Study of the Effect of Electrode Potential and Solution pH upon the Interfacial Behavior of 4-Pyridinecarboxaldehyde

Mark R. Anderson[†] **and Dennis H. Evans***[,‡]

Contribution from the Department of Chemistry, University of Utah, Salt Lake City, Utah 84112, and Department of Chemistry and Biochemistry, University of Delaware, Newark, Delaware 19716. *Received March 14, 1988. Revised Manuscript Received June 1, 1988*

Abstract: Surface-enhanced Raman scattering (SERS) spectra were obtained at a silver electrode in aqueous solutions at potentials from −0.2 to −0.6 V vs SCE and pH 1–7. The forms of 4-pyridinecarboxaldehyde that are adsorbed parallel those present in solution. In particular, the fraction of adsorbed species that is protonated at −0.2 V varies with pH in a manner almost identical with the fraction that is protonated in bulk solution. The protonated compound exists almost completely in the hydrated form (*gem*-diol) in the interface just as it does in solution. At a given pH, the fraction protonated on the surface increases as the potential is made more negative, a behavior attributed principally to enhanced adsorption of cationic species at negative potentials. In the presence of chloride, the fraction protonated decreases at the most negative potentials. This decrease is correlated with the desorption of chloride, suggesting that the pyridinium ion and chloride are adsorbed together. When the more strongly adsorbed bromide or iodide is used, the fraction protonated does not decrease at negative potentials.

A reactant molecule may exist in a variety of forms related to one another by acid–base reactions, complexation, tautomerization, etc. Frequently, one of these forms is more reactive than the others, causing the reaction to proceed via that particular species. A complete understanding of the reaction mechanism requires the identification of the reactive form, a task usually accomplished through a detailed evaluation of the reaction kinetics. When the reaction occurs at an interface (as in heterogeneous catalysis), it is highly desirable to have a very selective means of detecting adsorbed species while the reaction is occurring.

The reduction of aldehydes is an example of such a reaction. In aqueous solutions many aldehydes exist in two forms, the free aldehyde and the hydrate (*gem*-diol), with the relative concentrations being governed by a hydration equilibrium constant, K_h.

$$\mathrm{RCHO + H_2O = RCH(OH)_2}$$

$$K_h = [\mathrm{RCH(OH)_2}]/[\mathrm{RCHO}]$$

In the electrochemical reduction of such aldehydes, it is the free aldehyde that is the active form. In order for the *gem*-diol to be reduced, it must first dehydrate to form free aldehyde, which in turn is reduced at the electrode surface. The dehydration reaction, which is often the rate-limiting step, can occur in solution near the electrode or, possibly, on the electrode surface.

The electrochemical reduction of 4-pyridinecarboxaldehyde has been the subject of intense study.[1-7] In acidic media over 90% of the aldehyde is hydrated,[1] but it can be rapidly and efficiently reduced to the alcohol, 4-pyridylcarbinol.[6] The dehydration reaction has been shown to be a crucial feature of the reduction mechanism under a variety of solution conditions.[1-3,5,7] Though the dehydration is normally considered to occur only in solution near the metal surface, a significant fraction may react on the surface, a possibility enhanced by the strong adsorption of pyridine and its derivatives.

In order to investigate the adsorption of the free and hydrated forms of 4-pyridinecarboxaldehyde, a selective and sensitive method is needed. Surface-enhanced Raman spectroscopy (SERS) is an attractive candidate. In fact, the original observations of SERS were obtained with pyridine at a silver surface.[8-10] As later investigations demonstrated, SERS is unusually powerful for in situ investigation of metal–solution interfaces. The sensitivity is excellent and the information content of the spectra is high, permitting resolution and identification of very similar surface species. In this paper we report the application of SERS to the characterization of the various forms of 4-pyridinecarboxaldehyde adsorbed at silver surfaces as a function of solution pH and electrode potential. As will be seen, systematic investigation of the effects of these variables proved to be crucial in the detection of the adsorbed reactive free aldehyde, a species that was not

---

[†] University of Utah.

[‡] University of Delaware.

(1) Laviron, E. *Bull. Soc. Chim. Fr.* **1961**, 2325–2349.

(2) Blâzquez, M.; Camacho, L.; Jimênez, M.; Dominguez, M. *J. Electroanal. Chem. Interfacial Electrochem.* **1985**, *189*, 195–202.

(3) Camacho, L.; Blâzquez, M.; Jimênez, M.; Dominguez, M. *J. Electroanal. Chem. Interfacial Electrochem.* **1984**, *172*, 173–179.

(4) Rusling, J. F.; Zuman, P. *J. Org. Chem.* **1981**, *46*, 1906–1909.

(5) Rusling, J. F.; Zuman, P. *J. Electroanal. Chem. Interfacial Electrochem.* **1983**, *143*, 283–290.

(6) Nonaka, T.; Kato, T.; Fuchigami, T.; Sekine, T. *Electrochim. Acta* **1981**, *26*, 887–892.

(7) Bhatti, M.; Brown, O. R. *J. Electroanal. Chem. Interfacial Electrochem.* **1976**, *68*, 85–95.

(8) Fleischmann, M.; Hendra, P. J.; McQuillan, A. J. *Chem. Phys. Lett.* **1974**, *26* 163.

(9) Jeanmaire, D. L.; Van Duyne, R. P. *J. Electroanal. Chem. Interfacial Electrochem.* **1977**, *84*, 1–20.

(10) Albrecht, M. G.; Creighton, J. A. *J. Am. Chem. Soc.* **1977**, *99*, 5215–5217.

0002-7863/88/1510-6612$01.50/0